Pergamon

Carbon Vol. 36, No. 5–6, pp. 689–696, 1998

0008-6223/98 $19.00 + 0.00

PII: S0008-6223(98)00046-3

SCANNING TUNNELLING MICROSCOPY (STM) IMAGING OF CARBON NANOTUBES

L. P. Biró,[a,*] J. Gyulai,[a] Ph. Lambin,[b] J. B. Nagy,[b] S. Lazarescu,[b] G. I. Mark,[a] A. Fonseca,[b] P. R. Surján,[c] Zs. Szekeres,[c] P. A. Thiry[b] and A. A. Lucas[b]

[a]KFKI-Research Institute for Materials Science, P.O. Box 49, H-1525 Budapest, Hungary
[b]Institute for Studies in Interface Sciences, Facultés Universitaires Notre-Dame de la Paix, rue de Bruxelles 61, B-5000 Namur, Belgium
[c]Department of Theoretical Chemistry, Eötvös University, P.O. Box 32, H-1518 Budapest, Hungary

(*Received* 30 *October* 1997; *accepted in revised form* 4 *November* 1997)

Abstract—Carbon nanotubes prepared by thermal decomposition of hydrocarbons on supported Co catalysts were investigated by STM in air. An interpretation of the STM images is proposed which accounts for specific distortions taking place while scanning three-dimensional objects whose dimensions are of the order of the curvature radius of the tip. These distortions have both geometric and electronic origins, and cannot be neglected. The distortion mechanism was found to be different for nanotube diameters in the ranges of 1 nm and 10 nm. The 1 nm tubes are more strongly affected by their apparent broadening, reflecting the finite size of the tip apex. Here the distortion can reach up to 300% of the geometric diameter, whereas for 10 nm tubes the distortions are in the range of 50% of the geometric diameter. An apparent flattening of the nanotubes in the vertical direction was also found, which is attributed to differences in electronic densities of states between the substrate and the nanotube, and to an additional tunnelling barrier between the nanotube and the substrate. STM images with atomic resolution and line cut topographic profiles show similar structures as for the case of HOPG. However, the atomic corrugation was found to be five times smaller on the 1 nm diameter tubules than for the 10 nm family, the latter being close to the value obtained with HOPG. Coiled nanotubes have been imaged by STM for the first time. Here both the electrical resistance of the coiled nanotube and its elastic deformation play a significant role in the image formation process, these effects being more important than for straight nanotubes.

Key Words—A. Carbon nanotubes, A. catalytically grown carbon, C. scanning tunnelling microscopy (STM), D. electronic structure.

1. INTRODUCTION

Since their discovery by Iijima [1], carbon nanotubes have attracted the attention of researchers from various fields. An overview of the results obtained to date has been published recently [2]. Due to their remarkable versatility for studying objects with typical sizes in the range of 1–10 nm, scanning probe methods—scanning tunnelling microscopy (STM) [3] and atomic force microscopy (AFM) [4]—have been applied successfully to the investigation of these nano-objects. The carbon nanotubes which have undergone STM investigations can be grouped into two families: the 1 nm diameter range [5–8] and the 10 nm diameter range [9–12]. In some instances, atomic resolution imaging of the nanotubes has been achieved by several groups [6,9,10]. They found that the outer wall of the nanotubes exhibits a structure similar to that of highly oriented pyrolitic graphite (HOPG) when imaged by STM. In HOPG, only the so-called β sites—those atomic positions that do not have a C atom underneath—are observed by STM [13]. This effect is attributed to the interaction of the two outermost layers of graphite. It disappears when the latter are separated by intercalated molecules [14]. Therefore, the observed atomic structure is an indication that all nanotubes on which atomic resolution was achieved up to now were at least double-wall nanotubes.

One of the earliest and most complete experimental works on the characterisation of the electronic properties of carbon nanotubes was performed by Olk and Heremans [5]. Using scanning tunnelling spectroscopy (STS), these authors tried to correlate the gap values measured for semiconducting nanotubes with their apparent diameters. Their results show a linear relation with the reciprocal of the tube diameter, as expected theoretically, but with a slope different from that of theory. This discrepancy was attributed to possible chirality of the tubes and to the fact that the spectra were acquired in air.

The determination of the diameter of a carbon nanotube may raise some problems due to differences in the local density of states (LDOS) between the substrate and the nanotube, and due to convolution effects with the tip shape [15]. Without applying any correction for the above mentioned effects, it happens frequently that the measured apparent diameter is about two times the apparent height.

In the present paper, the mechanism of STM image

*Corresponding author. Fax: +36 1 395 9284; e-mail: biro@r1.atki.kfki.hu

formation for objects with dimensions comparable with the radius of curvature of the tip is briefly analysed, and corrections that have to be considered for extracting the diameter from the STM images are discussed. Atomic resolution images of straight nanotubes with diameter in the range of 1 nm and 10 nm are presented. In addition, the first STM images of a coiled nanotube are reported and the peculiarities of their image formation mechanism are discussed.

2. IMAGE FORMATION MECHANISM DURING IMAGING THREE-DIMENSIONAL OBJECTS WITH STM

Let us first consider a step on an atomically flat surface. This situation, frequently encountered on the cleaved surface of the HOPG, is sketched in Fig. 1(a). The shaded circle represents the apex of the STM tip, whereas the larger, concentric white ring around it shows the width of the tunnelling gap, Δ. When the tip comes close to the step, one may consider the atomically sharp step edge as imaging the tip while the "circle is rolling over the step". Therefore, the step will not appear atomically sharp in the image but will be "rounded". The rounding of the step contains valuable information concerning the shape of the tip. From Fig. 1(a), one can write the following relation between the apparent step width, L, and the other geometric quantities:

$$(\Delta + R)^2 = L^2 + (\Delta + R - h)^2 \qquad (1)$$

where h is the step height. It is useful to denote by $R_{\text{eff}} = \Delta + R$ the effective tip radius, which incorporates the tunnelling gap. With this notation, eqn (1) yields:

$$R_{\text{eff}} = \frac{L^2 + h^2}{2h} \qquad (2)$$

Knowing the value of R_{eff} from a HOPG step profile, one can determine the distortion introduced by the tip geometry in the apparent diameter of a cylindrical object, with radius $r < R_{\text{eff}}$, placed at a distance δ above the substrate, Fig. 1(b). In first approximation, we consider that the tunnelling probabilities (related to the LDOS) are similar over the substrate and the object. With this assumption, the distorted half-width of the object, $D_{\text{app}}/2$, becomes:

$$\frac{D_{\text{app}}}{2} = \sqrt{(2R_{\text{eff}} - \delta)(2r + \delta)} \qquad (3)$$

As eqn (3) shows, the value of $D_{\text{app}}/2$ measured experimentally depends on the effective tip radius (through this, it depends on the width of the tunnelling gap, i.e. on the value of the LDOS) and on the spacing δ between the object and the supporting surface. These dependencies have frequently been neglected in the interpretation of STM images of the nanotubes. For the particular case of a carbon nanotube on HOPG, δ can be estimated to be 0.34 nm as representing either the interplanar spacing in graphite or the distance between individual nanotubes in the ropes of single wall nanotubes (SWNT) [16]. On other substrates, other values of δ may be found.

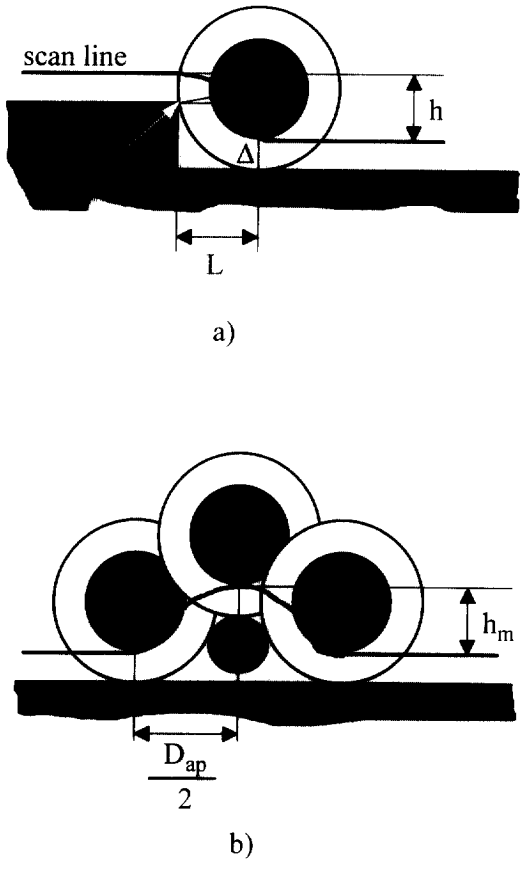

Fig. 1. Schematic presentation of an STM tip: shaded sphere of radius R encircled by white ring of thickness Δ, the tunnelling gap. (a) Imaging a cleavage step on the surface of HOPG; (b) imaging a cylindrical object placed at a distance δ over the support.

3. EXPERIMENTAL RESULTS AND DISCUSSION

The work was carried out with carbon nanotubes prepared by decomposition of acetylene at 700°C over supported transition metal catalysts [17,18]. Two types of samples were prepared by ultrasonication in toluene of the nanotube containing material, as reported earlier [15]. A-type samples were prepared directly from the material purified from the catalyst [17]. B-type samples followed the same procedure except that a wet oxidation was realised to remove the amorphous fraction [17] before ultrasonication. For all the samples, the suspension obtained after ultrasonication was deposited on freshly cleaved HOPG and the solvent was left to evaporate at room temperature. In A-type samples both nanotubes with 1 nm and 10 nm were found with STM, while in B-type samples only nanotubes of the 10 nm diameter family were found. This is an indication that the wet oxidation destroys the small diameter nanotubes.

The STM images were acquired in constant-current mode, using tunnelling currents in the range 0.2–1 nA, bias voltages in the range 0.1–1 V, and scan frequencies of 1–2 Hz. Mechanically prepared Pt tips were used, the radius of curvature of which was checked with respect to the HOPG surface.

A large area of an STM scan of a step with height of four atomic layers is shown in Fig. 2(a). The line cut taken along the line marked in the upper part of the image is shown in Fig. 2(b), from which the effective tip radius could be estimated to be $R_{\text{eff}}=4.05$ nm. Fig. 3(a) shows a region where, after cleaving the HOPG, pieces of graphene layers already separated from the underlying layers were folded back on the higher terrace to which they were bounded by van der Waals interaction. The regions where these graphene layers are folded back have a cylindrical shape and are imaged as bright bands. This is the result of the finite value of their curvature radius. The AFM and STM observation of similar features has been reported earlier by Hiura *et al.* [19]. The interesting objects for our present study are the three fainter features situated on the lower terrace which we identify as being nanotubes. These

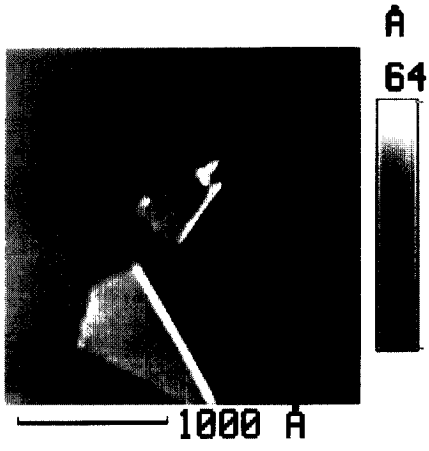

a)

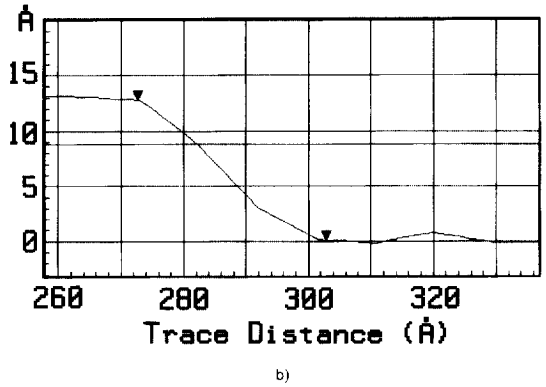

b)

Fig. 2. Large-scale STM image of a step on the surface of HOPG: (a) folded graphene sheets (lighter objects) and carbon nanotubes (fainter objects) (b) line cut taken along the line marked in (a).

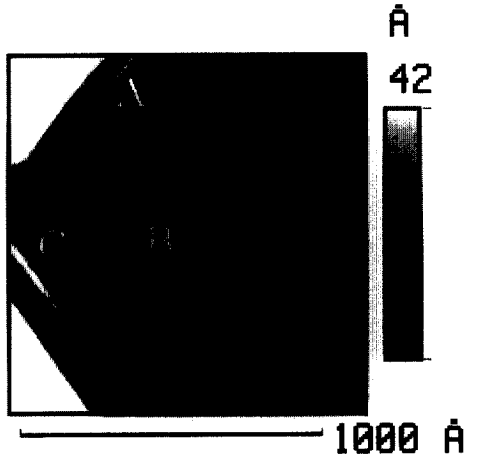

a)

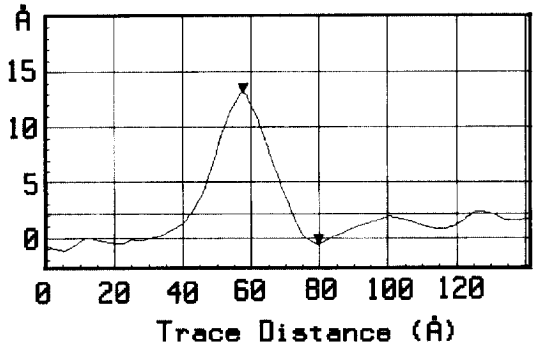

b)

Fig. 3. Physically zoomed detail of Fig. 2: (a) the objects marked A and C do not exhibit structural details, object B is a "raft" of nanotubes; (b) line cut taken across object A along the line marked in (a).

are aligned parallel to each other, or make an angle close to 120°; we interpret that their positions are not random, but nanotubes tend to be aligned with the underlying HOPG substrate.

Figure 3(a) is a physically zoomed detail of the region shown in Fig. 2(a) (i.e. not a simple blow up obtained by software). One can notice that two of the objects, labelled A and C, do not show structural details, whereas B looks like a "raft" of nanotubes, like the ones reported earlier [15]. The line cut taken through the isolated nanotube A is given in Fig. 3(b). One can deduce from this the ratio $(D_{\text{app}}/2)/h_{\text{m}}=1.6\pm0.2$, where h_{m} is the measured height (see Fig. 1(b)). A physically zoomed detail (Fig. 4(a)) of the raft B is used for investigating the question of the diameter distortion with more details. Calculating the ratios of D_{app} to h_{m} for the two tubes on both sides of the raft gives 2.58 for the tube on the left side, and 3.16 for the tube on the right side. Comparing the ratios of D_{app} to h_{m} leads us to the conclusion that the distortion is stronger for the smaller diameters. This finding is in agreement with the fact that the discrepancy between theoretical and

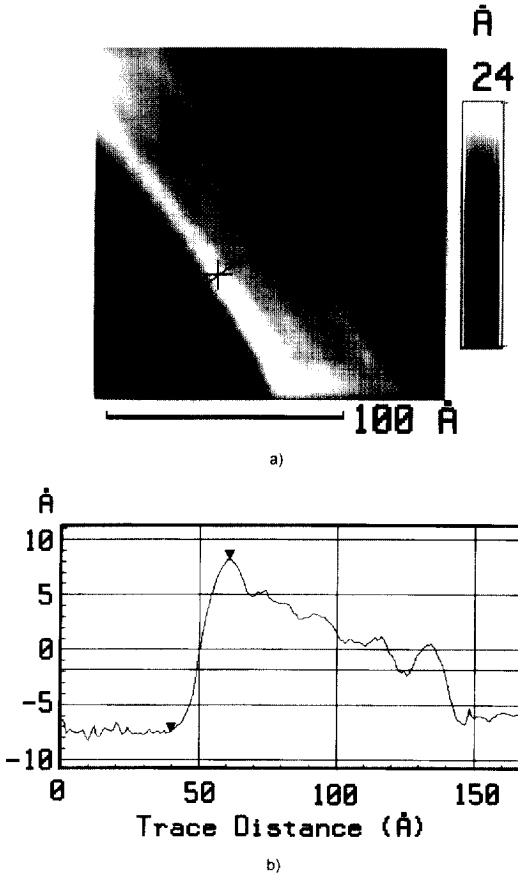

Fig. 4. Physically zoomed detail of Fig. 3: (a) raft of nanotubes with diameters in the range of 1 nm; (b) line cut along the line marked in (a).

measured data [5] is greater for the small nanotube diameters.

The nanotube at the centre of the raft shown in Fig. 4(a) is a good candidate for determining its real diameter value. Indeed, the width of the tube placed centrally in a raft-like stack of similar nanotubes should appear correctly in the image. With this in mind, the diameter of the central tube from the raft can be extracted from Fig. 4(b), $D=1.28$ nm. Comparing this value to the height h_m of the same tube, 1.06 nm, one can calculate the distortion in the height due to the different tunnelling probabilities over the HOPG and over the nanotube. The geometrically correct height, $h=\delta+D=1.62$ nm, is greater than the experimentally measured value by 0.56 nm. The difference can be of two-fold origin: first, the LDOS over the nanotube differs from that over the HOPG; second, even if the LDOS values coincide, the tube is not an integral part of the HOPG and, instead of having one single tunnelling gap between the tip and the nanotube, there is a second tunnelling gap between the nanotube and the HOPG, as shown in Fig. 5(a, b). To analyse in more detail the consequences of the second tunnelling gap, we have studied the effects of the geometry on the tunnelling of an electron from

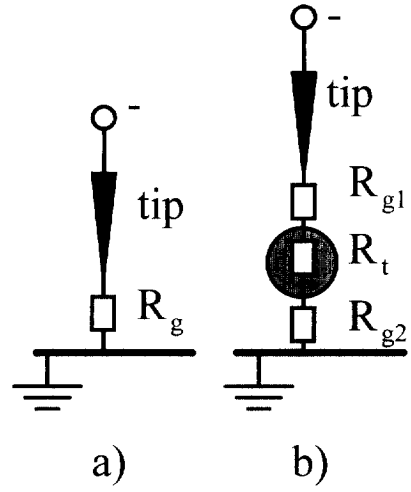

Fig. 5. Schematic representation of nanotubes over the substrate: (a) a regular array, (b) equivalent tunnelling circuit in the absence of the nanotube, (c) equivalent tunnelling circuit with the nanotube "floating" over the support.

the tip through the nanotube to the sample by a dynamical one-particle wavefunction calculation. In the first approximation a simple model was used, which takes into account only the geometry of the objects involved in the tunnelling process. An infinitely small bias was assumed. The time development of the (quantum mechanical) probability density $\rho(x, z, t)$ (Fig. 6) is calculated from the $\Psi(x, z, t)$ solution of the time dependent Schrödinger equation which was solved numerically [20]. The simple model potential is derived from the assumption that the electron moves freely inside the tip, and the HOPG, and inside the wall of the nanotube. The work function is taken to be 2.49 eV and the Fermi energy 2.31 eV [21]. The jellium surface is assumed to be at 0.71 Å distance from the geometrical surface of the electrodes. The detailed simulation [22], from which selections are presented in Fig. 6, shows that due to the presence of the second tunnelling gap a significant fraction of the wave packet is reflected back to the tip, i.e. the reduction of the tunnelling current occurs even when the differences in the LDOS values of the support and of the nanotube are not taken into account.

The observation of "raft-like" arrangements like that shown in Fig. 4(a) and those reported earlier [15], or the "rope-like" [16] arrangement of carbon nanotubes, suggests an ordering mechanism responsible for the growth of the tube arrays constituted of tubes with diameters in the 1 nm range. The effect of intertube van der Waals interaction was analysed using the potential given in ref. [23]. The strain energy per carbon atom due to bending was estimated by *ab initio* quantum chemical Hartree–Fock calculations in minimal STO-3G basis set on a naphthalene molecule. By a fitting procedure, the E_{bending}/N relationship was established:

$$\frac{E_{\text{bending}}}{N} = 3.13995 \times 10^{-5}\alpha \text{ [eV/deg]} \qquad (4)$$

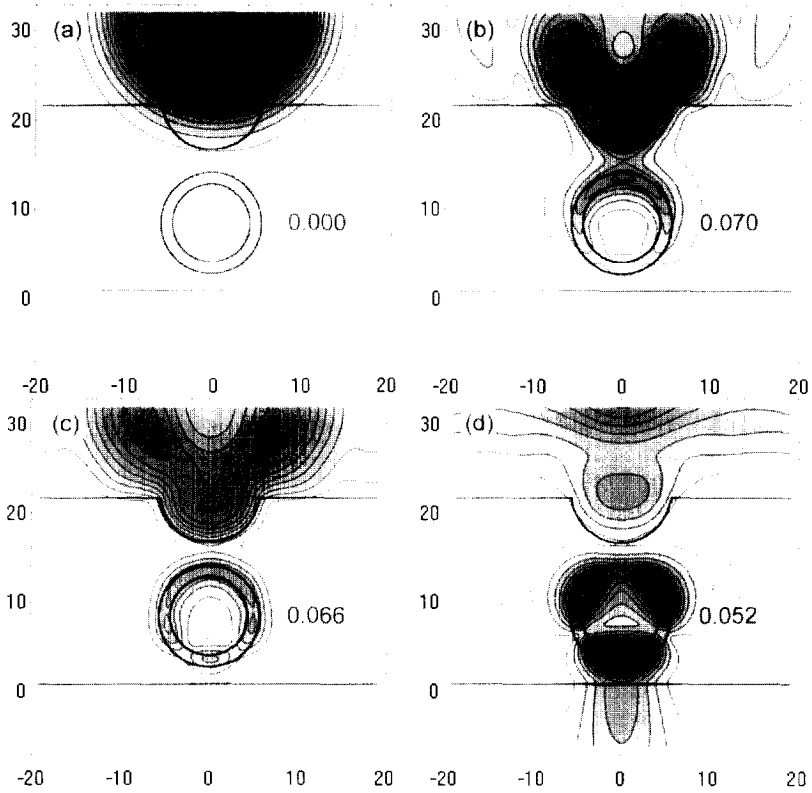

Fig. 6. Selections from the detailed simulation of tunnelling through a section of a nanotube 1 nm in diameter floating over the substrate. The scales are given in ångströms. The wave packet is supposed to propagate freely in the tip modelled as a semi-circle attached to a semi-infinite plane, through the nanotube, and through the support considered as a semi-infinite plane. The distribution of the probability density of the particle is plotted: (a) the wave packet is launched at time "0" from the bulk of the tip; (b) after 0.85 fs; (c) after 1.98 fs; (d) after 3.04 fs. Each image is normalised to the maximum probability density found in the observation window. The fractions of the total probability density found in the observation window are: (a) 0.48; (b) 0.88; (c) 0.62; (d) 0.09. The numerical values indicated in the images show the fraction of the probability found in the tube region.

where N is the number of C atoms and α is the bending angle. The van der Waals intertube interaction was calculated using a hexagonal close-packed arrangement of nanotubes, if viewed along their axis. The value of the intertube distance was found to be around 0.33 nm, in good agreement with experimental values of 0.34 nm, and showed no significant dependence on the diameter of the nanotubes. Relatively large diameter values, in the range of 2 to 3 nm, were obtained by optimising the energy of the tube array. This shows that the mere van der Waals interaction is not sufficient to explain the growth of the arrays of nanotubes with diameters in the range of 1 nm. Using a semi-empirical all-valence electron CNDO/2 calculation [24], a simple model, based on the intratube bonding interactions in short tubes — obtained by folding of "sheets" of fused together hexagonal carbon rings constituted of 20, 32, 40, 52, 72, and 92 C atoms — yielded a similar optimal diameter value for the most stable tubules, in the range of 1 nm, as those reported by Thess *et al.* [16]. The factor which favours short radii is the attractive interaction between two-neighbour carbon atoms at the open tube endings. The values of total energy per C atom, E/N, for different tube radii indicate as most stable ones the nanotubes with radius of 4.52 Å ($E/N = -6.92394$ eV) and 5.87 Å ($E/N = -6.92341$ eV).

At this point of the discussion, two geometrical distortions have been put in evidence: the one originating from the tip-shape convolution which broadens the apparent horizontal width of the objects, and *the one from the variations of the LDOSs which* reduces the apparent height of the nanotube. The first distortion enlarges the apparent diameter of a nanotube by a factor of as much as 3. By comparison, the relative error introduced by the second was only $0.56/1.62 = 0.34$ in the example discussed previously. As discussed earlier [15], the most advantageous situation is when a bundle is composed of more than one layer of nanotubes. Then the vertical distortion is reduced by the fact that the topmost tubes are placed on a similar support.

In the case of nanotubes with a diameter of the order of 10 nm, the most important distortions may arise from the deviations of the shape of the tip over the last 10–20 nm from that of an idealised "geometric line". Let the tip be modelled by a cone pointing

towards the measured surface. The cone, with its apex at a distance Δ from the substrate surface, comes in lateral (tunnelling) contact with the nanotube of radius r at a point that is situated at $H = [r(1+\sin\beta/2) - \Delta(1-\sin\beta/2) + \delta]$ on the vertical axis of the cone, where β is the cone angle. The radius of the cone at this height is $R_c = H \operatorname{tg}\beta/2$. The value of R_c will be added to the measured tube width on both sides. The distortion produced on the measured diameter of a nanotube with a diameter of 10 nm by a tip with $\beta = 20°$ will be $2 \times 1.85 = 3.7$ nm, i.e. 37%. The distortion shall increase as the real tip shape deviates from a cone. Remark also that realistic cone angles are larger than 20°. In the vertical direction, a reduction of the apparent tube height due to the causes already discussed for the nanotubes with 1 nm diameter introduces an error of 5.6%. Again, if no detailed image analysis is done, the measured height is a better approximation for the diameter of the nanotube.

In atomic resolution imaging achieved by STM, the normal corrugation amplitude found on HOPG is in the range of 0.1 nm [25]. We found values in this range for the HOPG substrate on which the nanotubes were deposited. When the vertical dimension of the object being scanned is of the order of 1 nm, only moderate chances exist to achieve atomic resolution during the same scan over the substrate and over the object, too. The atomic resolution images reported so far on nanotubes have been obtained on nanotubes with relatively large diameters, 3.5 nm [6] and 16 nm [10]. The atomic resolution images were confined to a vicinity of the topmost part of the nanotube. Unfortunately, no line cuts have been published showing the atomic corrugation. Figure 7(a, b) show an atomic resolution image obtained on a detailed part of a nanotube raft together with a corresponding line cut. The line cut is taken along the line on which the two crosses are seen, the other line was drawn parallel to the tube axis as a guide. The chiral angle deduced from the angle between the two lines is 4°. The distance between the two markers on the line cut is 0.244 nm and the corrugation amplitude is 0.02 nm, this value being significantly smaller than for HOPG. As one can see from Fig. 7(a), the diameters of the nanotubes composing the raft are in the 1 nm range, the largest tube on which the line cut was taken has a diameter of 1.6 nm. For comparison, an image with atomic resolution obtained on a nanotube with 8.8 nm diameter is shown in Fig. 8(a, b). The three characteristic axes for HOPG are marked by black lines on the STM image, a slight distortion of the equilateral triangle is observed, which is due to drift during the acquisition of the image. The line cut taken along the line marked by A shows the expected corrugation in the range of 0.1 nm, while the distance of successive maxima is 2.55 nm. Further, systematic investigations are needed to decide if the lower corrugation amplitude found on the 1.6 nm diameter tube is connected

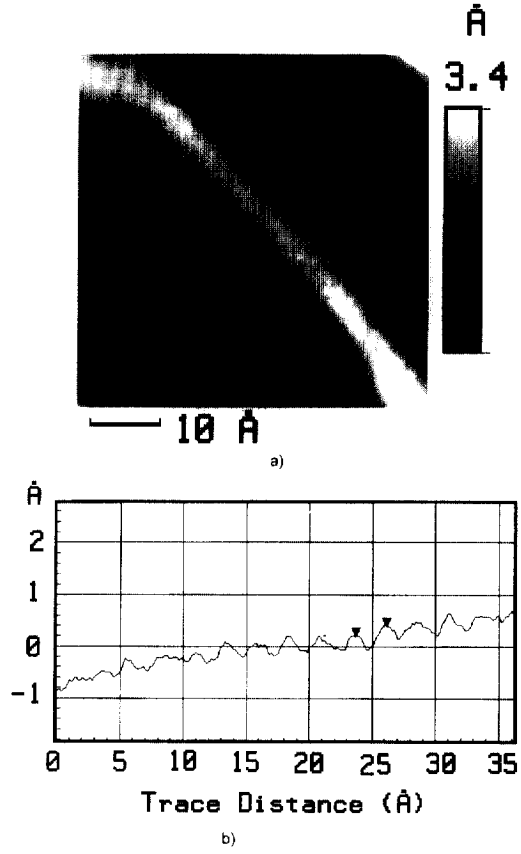

Fig. 7. Atomic resolution STM image of a detail of a "raft" of nanotubes, $I_t = 0.24$ nA, $U_b = 0.41$ V: (a) plan view image, the central tube has a diameter of 1.6 nm; (b) line cut along the black line in (a) which is marked by two crosses.

with the greater curvature of the graphene layers, which may influence the interaction between the graphene sheets.

The coiled nanotubes produced by the catalytic method [26] are really challenging objects for STM imaging. In addition to the usual geometric and electronic factors, elastic properties specific of the coil may add a contribution. Figure 9(a) shows the STM image of what we believe is such an object. Figure 9(b) shows a line cut running through the upper part of a coil element. After the first region, where the apparent height increases while the tip starts "climbing" onto the nanotube, a dip follows in the line cut. This behaviour was reproduced all over the coiled nanotube. Two effects may account for this, either individually or in combination. First, the coil, by contrast with a straight nanotube, makes "contacts" with the substrate only at discrete points spaced by a distance equal to the period p of the coil, which for this particular coiled nanotube is $p =$ 14.02 nm. The charges can flow to the substrate only through these contact points, so that the electrons will have to move along the tube. This means that the resistivity of the tube is at a maximum in the topmost region of the coil. Second, the upper part

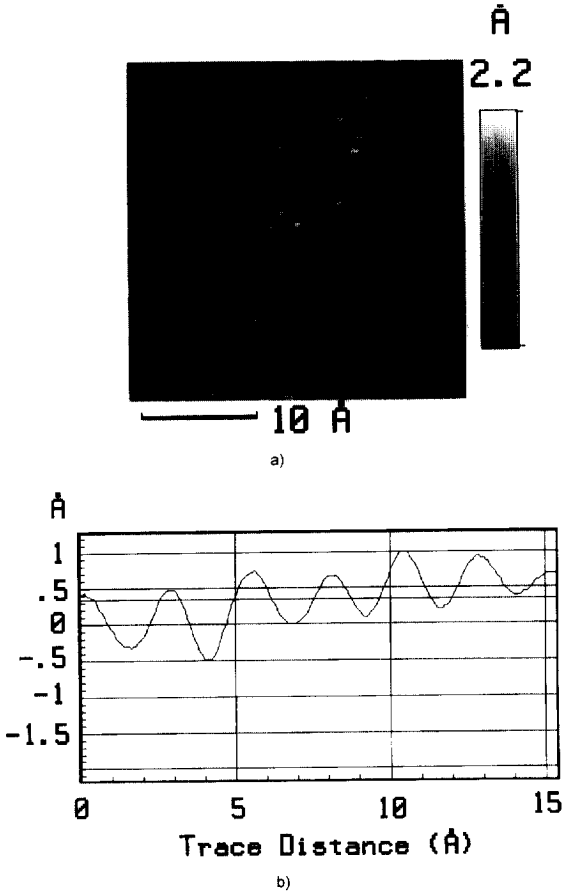

Fig. 8. Atomic resolution image on a multi-wall nanotube with a diameter of 8.8 nm, $I_t = 0.26$ nA, $U_b = 0.49$ V: (a) the direction of the three main axes characteristic of STM images of HOPG are marked; (b) the line cut taken along the line marked by A in (a).

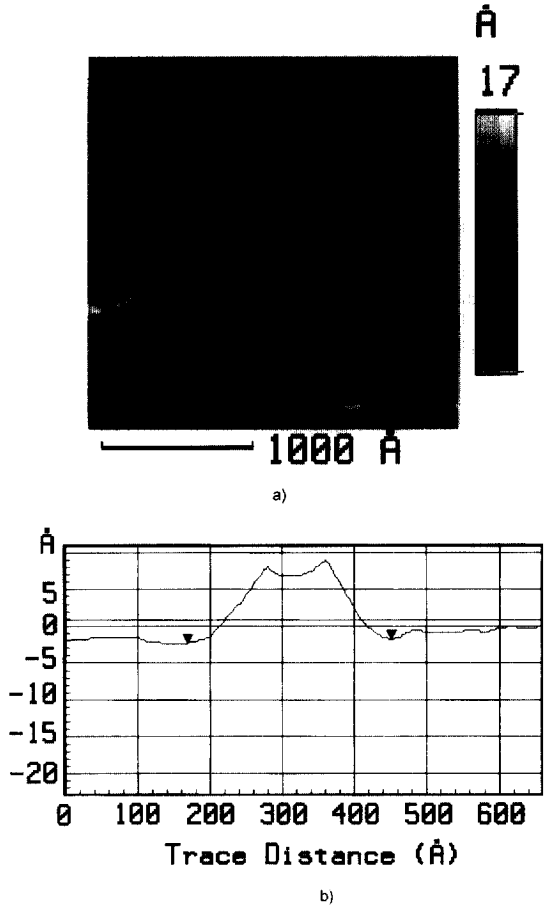

Fig. 9. STM image showing a coiled carbon nanotube: (a) detail zoomed by software from an image of 1 μm^2; (b) line cut along the line indicated in (a), note the dip in the topmost region of the coiled nanotube, where the mere topography should yield a maximum.

of the coil may suffer elastic deformation when the tip is passing over it. Further detailed studies are needed to determine which contribution is more important. The "dip effect" was not found on those coiled nanotubes which were not supported on the HOPG, but were criss-crossing each other. This may be an indication for the dominance of the deformation in dip production.

4. CONCLUSIONS

The mechanism of STM image formation when scanning three-dimensional objects with dimensions of the order of the effective curvature radius of the tip was analysed. This analysis was applied to the detailed study of distortions which may affect the diameter of carbon nanotubes as measured from an STM image. The distortion resulting from geometric and electronic effects, and from the fact that the nanotubes "float" over the surface of the support, may not be neglected.

The mechanism of the distortion is different for the nanotubes in the diameter ranges of 1 nm and 10 nm. The 1 nm tubes are more strongly affected by the apparent broadening. Here the distortion can reach values up to 300% of the geometric diameter, whereas for 10 nm tubes the distortions are in the range of 50% of the geometric diameter. The apparent flattening in the vertical direction is attributed to the differences in LDOS between the substrate and the nanotube, and to the existence of two additional resistances in the tunnelling circuit: the resistance of the nanotube itself, and the resistance of the second tunnelling gap between the nanotube and its support.

The atomic resolution images on carbon nanotubes and the line cut topographic profiles show similar structure as for the case of HOPG. However, corrugation values were found lower for the 1 nm diameter family than for the 10 nm family, the latter being close to the value obtained with HOPG.

Coiled nanotubes have been imaged by STM for the first time. The images and the line cuts indicate that both the resistance of the nanotube and its elastic deformation play a significant role in the

image formation process, and these effects are more important than in the case of the straight nanotubes.

Acknowledgements—Part of this work was performed within the Inter-University Research Program on Reduced Dimensionality Systems (PAI/IUAP No. 4/10) initiated by the Belgian State Government. The work has been partly supported by the EC TMR Research Network NAMITECH ERBFMRX-CT96-0067 (DG12-MIHT) in Belgium, and by AKP Grants 96/2-637 and 96/2-462 in Hungary. L. P. Biró acknowledges the financial support of the CGRI of the French Community of Belgium and of the FUNDP, Namur, Belgium. P. R. Surján acknowledges support from the Grants OTKA T021179, T023052, and MKM 183/96.

REFERENCES

1. Iijima, S., *Nature*, 1991, **354,** 56.
2. Dresselhaus, M. S., Dresselhaus, G. and Ecklund, P. C., *Science of Fullerenes and Carbon Nanotubes.* Academic Press, San Diego, 1996.
3. Binning, G., Rohrer, H., Gerber, Ch. and Weibel, E., *Phys. Rev. Lett.*, 1982, **49,** 57.
4. Binning, G., Quate, C. and Gerber, C. H., *Phys. Rev. Lett.*, 1986, **56,** 930.
5. Olk, C. H. and Heremans, J. P., *J. Mater. Res.*, 1994, **9,** 259.
6. Ge, M. and Sattler, K., *Science*, 1993, **260,** 515.
7. Ge, M. and Sattler, K., *J. Phys. Chem. Solids*, 1993, **54,** 1871.
8. Sattler, K., *Carbon*, 1995, **33,** 915.
9. Xie, S., Li, N., Zhang, Z., Lu, W., Wang, G., Qian, S. and Fu, C., *J. Mater. Sci.*, 1995, **30,** 2291.
10. Lin, N., Ding, J., Yang, S. and Cue, N., *Carbon*, 1996, **34,** 1295.
11. Zhang, Z. and Layber, C. M., *Appl. Phys. Lett.*, 1993, **62,** 2792.
12. Rivera, W., Perez, J. M., Ruoff, R. S., Lorents, D. C., Malhotra, R., Lim, S., Rho, Y. G., Jacobs, E. G. and Pnizotto, R. F., *J. Vac. Sci. Technol. B*, 1995, **13,** 327.
13. Tománek, D., Louie, S. G., Mamin, H. J., Abraham, D. W., Thomson, R. E., Ganz, E. and Clarke, J., *Phys. Rev. B*, 1987, **35,** 7790.
14. Olk, C. H. and Heremns, J., *Phys. Rev. B*, 1990, **42,** 7524.
15. Biró, L. P., Nagy, J. B., Lambin, Ph., Lazarescu, S., Fonseca, A., Thiry, P. A. and Lucas, A. A., in: *11th Int. Winterschool on Electronic Properties of Novel Materials*, 1–7 March 1997, Kirchberg, Austria. World Scientific, Singapore, in press.
16. Thess, A., Lee, R., Nikolaev, P., Dai, H., Petit, P., Robert, J., Xu, C., Lee, Y. H., Kim, S. G., Rinzler, A. G., Colbert, D. T., Scuseria, G. E., Tomanek, D., Fischer, J. E and Smalley, R. E., *Science*, 1996, **273,** 483.
17. Fonseca, A., Hernadi, K., Nagy, J. B., Bernaerts, D. and Lucas, A. A., *J. Mol. Catal.*, 1996, **107,** 159.
18. Hernadi, K., Fonseca, A., Nagy, J. B., Bernaerts, D., Fudala, A. and Lucas, A. A., *Zeolites*, 1996, **17,** 416.
19. Hiura, H., Ebbesen, T. W., Fujita, J., Tanigaki, K. and Takada, T., *Nature*, 1994, **367,** 148.
20. Feit, M. D., Fleck, J. A. and Steiger, A., *J. Comput. Phys.*, 1982, **47,** 12.
21. Márk, G. I., Dynamical calculation of tunnel current for STM, in: *NANO IV, Fourth Int. Conf. on Nanometer-Scale Science and Technology*, 8–12 September 1996, Beijing, China, p. 186.
22. The complete simulation is accessible at: http://www.phy.bme.hu/pub/emrs97/index.html
23. Girifalco, L. A. and Lad, R. A., *J. Chem. Phys.*, 1956, **25,** 693.
24. Pople, J. A. and Beveridge, D. L., *Approximate Molecular Orbital Theory*. McGraw-Hill, New York, 1970.
25. Binning, G., Fuchs, H., Gerber, Ch., Rohrer, H., Stoll, E. and Tosatti, E., *Europhys. Lett.*, 1986, **1,** 31.
26. Zhang, X. B., Zhang, X. F., Bernaerts, D., Van Tendeloo, G., Amelinckx, S., Van Landuyt, J., Ivanov, V., Nagy, J. B., Lambin, Ph. and Lucas, A., *Europhys. Lett.*, 1994, **27,** 141.